Microphase Separation and Crystallization in an Asymmetric Diblock Copolymer: Coupling and Competition

Liangbin Li,[†] Yaelle Séréro,[†] Michel H. J. Koch,[‡] and Wim H. de Jeu*,[†]

FOM-Institute for Atomic and Molecular Physics, Kruislaan 407, 1098 SJ Amsterdam, The Netherlands, and European Molecular Biology Laboratory, EMBL c/o DESY, Notkestrasse 85, D-22603, Germany

Received July 19, 2002
Revised Manuscript Received December 10, 2002

Coupling and competition between different phase transitions have been widely applied to create ordered structures over various length scales and may hold the key to the development of new structures and advanced devices.[1,2] In this context, the richness of phase transitions in polymers, as well as their mutual coupling, provides an inexhaustible source for material science. In general, two kinds of coupling between phase transitions can be found in polymer systems. In the case of static coupling two phase transitions occur sequentially, separated in time or by different external fields such as pressure and temperature. Alternatively, two phase transitions may take place at the same conditions with comparable kinetic rates, which can be regarded as a case of dynamic coupling. A typical example of such a system is a block copolymer with an amorphous block and a crystallizable or liquid-crystalline one.[3−10] The inherent complexity of amorphous block copolymers, which self-organize into lamellar, cylindrical, or other microphase-separated structures because of incompatible AB or ABC blocks,[11−13] is greatly increased by such a second phase transition. The final phase structure and crystalline morphology in amorphous−crystalline block copolymers depend on the competition between three phase transitions, i.e., the order−disorder transition of the diblock copolymer, the crystallization of the crystallizable block, and the vitrification of the amorphous block. Depending on the order−disorder transition temperature T_{ODT}, the melting temperature T_m, and the glass transition temperature of amorphous block T_g, both unconfined and confined crystallizations have been observed. The possible phase behavior is shown in Figure 1, in which a generic block copolymer phase diagram is combined with three typical melting lines for the crystallizable block. The increase of the melting temperature with the volume fraction of the crystallizable block is based on Flory's copolymer theory.[14] Note that a modulated phase and a gyroid phase may exist between the lamellar and cylinder phases.[15] For unconfined crystallization (region a), the phase separation between the blocks is driven by crystallization of the crystallizable block, resulting in alternating crystalline and amorphous lamellae.[16,17] For crystallization within the ordered-phase morphology (region c), the crystallization may either occur within or break out of the ordered confining boundaries.[5−10,18,19] In regions a and c, in general any coupling of the two phase transitions is expected to be static. In contrast, in region b both the crystallization and the order−disorder transition rates are relatively slow with comparable rates. Now dynamic coupling and kinetic competition between crystallization and microphase separation can be expected, possibly resulting in some interesting morphologies. In low-molecular-weight block copolymers both transitions have to overcome an energy barrier for nucleation, and the mutual coupling may promote nucleation. After nucleation, kinetic competition during the growth process determines the final morphology. In a symmetric diblock copolymer both the crystallization and the microphase separation lead to the formation of lamellae. However, for asymmetric block copolymers the competition between lamellae, driven by crystallization, and cylinders or spheres, driven by the microphase separation, may create new ordered structures. In this communication we present an example of such a coupling and competition corresponding to region b of Figure 1. At large supercooling, the crystallization dominates the domain growth resulting in lamellar stacks, while at low supercooling the kinetic rates of the two processes are comparable, leading as a compromise to a hexagonal perforated lamellar phase.

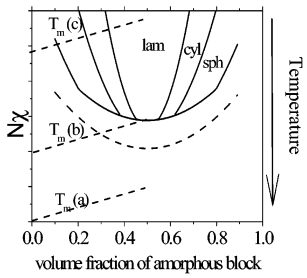

Figure 1. Schematic phase diagram of a block copolymer with one crystallizable block.

An asymmetric poly(ethylene oxide)-*b*-polystyrene (PEO-*b*-PS) diblock copolymer was used, with molecular masses of 3000 g/mol for PEO and 1000 g/mol for the PS block as supplied by Goldschmidt AG (Essen Germany). The values of T_m and T_{ODT} are comparable: T_m as determined from our SAXS measurements is about 54 °C, while T_{ODT} as reported from neutron scattering and rheology[20] varies from 64 to 70 °C. The system was studied by simultaneous small- and wide-angle X-ray scattering (SAXS and WAXS). A conventional rotating anode source was used with an area detector and linear detector for collecting the SAXS and WAXS intensity, respectively.[21] Additional time-resolved SAXS−WAXS measurements[22] were made at EMBL beamline X33 of HASYLAB (DESY, Hamburg).[23]

Typical SAXS and WAXS patterns of PEO-*b*-PS during isothermal crystallization at 45 °C are shown in Figure 2. The intensity is displayed as a function of $q = 4\pi \sin\theta/\lambda$, the modulus of the wave vector transfer **q**, where $\lambda = 0.15$ nm is the X-ray wavelength and 2θ the scattering angle. Up to crystallization temperatures of 49 °C the SAXS and WAXS peaks appear simultaneously, which indicates that the order−disorder transition does not occur prior to the crystallization. During heating they also disappear simultaneously, confirming that crystallization induces the phase separation. Integrated one-dimensional SAXS profiles of PEO-*b*-PS crystallized at different temperature are shown in

[†] FOM-Institute for Atomic and Molecular Physics.
[‡] European Molecular Biology Laboratory.
* Author for correspondence: e-mail dejeu@amolf.nl.

10.1021/ma025602c CCC: $25.00
Published on Web 01/17/2003

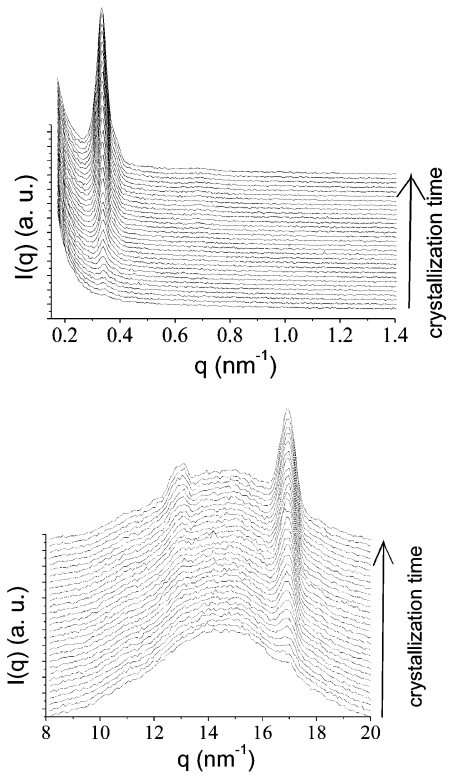

Figure 2. One-dimensional SAXS and WAXS patterns of PEO-*b*-PS during crystallization after an induction period of about 2 h, 2 min/frame, 4 min intervals.

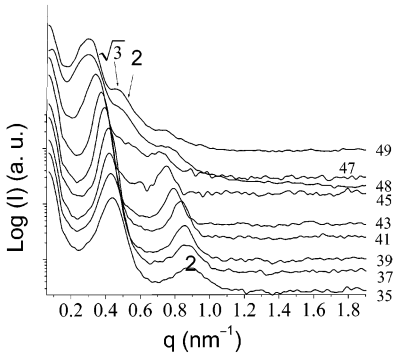

Figure 3. One-dimensional SAXS patterns of PEO-*b*-PS crystallized at different temperatures. The crystallization temperature is indicated in °C.

Figure 3. With increasing crystallization temperature the position of the first-order SAXS peak shifts continuously to lower wave vectors. After crystallization below 47 °C, the q value of the second-order peak is exactly twice that of the first-order one, indicating the formation of lamellae. Figure 4 gives the long period and full width at half-maximum (fwhm) of the first-order SAXS peak of Figure 3. The long period monotonically increases with temperature, while the fwhm has a minimum for the sample crystallized at about 43 °C. The temperature dependence of the long period is consistent with polymer crystallization theory.[24] Above 43 °C, the decrease of intensity of the second-order peak and the increase of the fwhm indicate a less ordered packing of the domains. A rather different morphology was obtained at higher crystallization temperatures (48 and 49 °C). Now peaks are observed at $\sqrt{3}$, 2 times the fundamental wave vector, indicating hexagonal symmetry. From these results we cannot decide on either cylinders or hexagonal perforated lamellae (HPL).

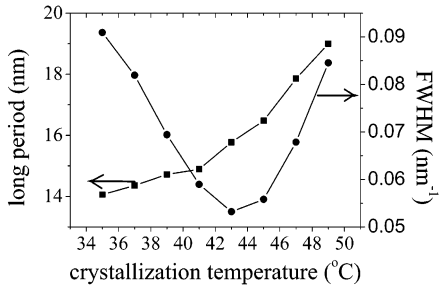

Figure 4. Long period and fwhm of the first-order maximum from Figure 3.

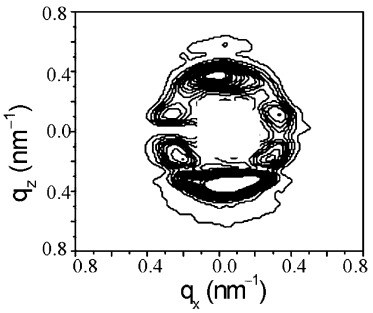

Figure 5. Contour plot of a two-dimensional SAXS pattern perpendicular to the X-ray beam of PEO-*b*-PS crystallized at 49 °C.

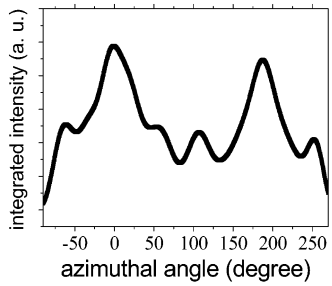

Figure 6. Azimuthally integrated intensity distribution of the pattern of Figure 5 over the range $0.22 \leq q \leq 0.45$ nm^{-1}.

A two-dimensional SAXS pattern of a sample crystallized at 49 °C is presented in Figure 5, which indicates oriented domains. This is attributed to their slow growth as no preorientation was imposed on the sample externally. The X-ray beam is perpendicular to the layer normal, which reveals the interlayer spacing as well as an in-plane view of the hexagonal structure. The two strong meridianal maxima in the scattering can be attributed to lamellae, while the four off-equatorial maxima indicate an ABAB packing of hexagonal perforations in the lamellae.[26,30] Their spacing is about 21 nm, i.e., approximately 1.15 times the lamellar spacing of about 18.5 nm. This picture is very similar to neutron scattering results of HPL phases.[26] The intensity distribution integrated in the azimuthal direction over the range of $0.22 \leq q \leq 0.45$ nm^{-1} is shown in Figure 6. The angle between the meridian and the off-equatorial maximum is approximately 55°, which is also consistent with the HPL structure.

The X-ray evidence of the formation of a perforated lamellar structure is substantiated by atomic force microscopy (AFM). A 0.5 mm thick spin-coated film was crystallized at 48 °C for 96 h under nitrogen. At this large thickness the structural features are close to those of the bulk material. AFM measurements in the semicontact mode were performed on the native surface at room temperature (Figure 7). The picture shows lamel-

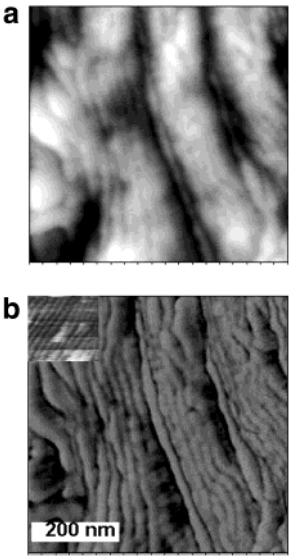

Figure 7. AFM height (a) and phase (b) image of PEO-*b*-PS crystallized at 48 °C. The inset shows perpendicular lamellae at 47 °C.

lar structures, particularly pronounced in the phase image, and somewhat tilted with respect to the layer normal. The inset in Figure 7b shows a view of normal lamellae crystallized at 47 °C. The observed modulations in the lamellae indicate their perforation. The somewhat larger spacing as compared to the SAXS values can be attributed to the tilt. The smearing effect due to relative large tip curvature radius (about 15 nm) is another reason.

The HPL phase has been observed previously between the hexagonal cylinder and the lamellae phase in some short-chain block copolymers.[25−29] Simulations and experimental findings suggest that the HPL phase is induced by mechanical shear and is a nonequilibrium, long-lived metastable or intermediate phase.[28,29] Shear deformation, e.g. during spin-coating, plays an important role in its formation and stability.[30] In the present case, the coupling and competition between crystallization and the microphase separation determine the formation of the HPL phase.

From the thermodynamic point of view, crystallization is a strongly first-order transition whereas the order−disorder transition is weakly first-order and fluctuation-induced. Although some studies of the kinetics of the order−disorder transition exist, a direct quantitative comparison with crystallization is difficult, especially for asymmetric systems.[31,32] It is, however, possible to describe the energy barrier ΔG* for the two processes by similar equations, assuming that the nuclei for microphase separation are spherical and those for crystallization are lamellar:[33]

$$\Delta G^*_{\mathrm{ODT}} = \frac{16\pi\sigma^3 (T^\circ_{\mathrm{ODT}})^2}{3\Delta h_{\mathrm{ODT}}^2 (T^\circ_{\mathrm{ODT}} - T_x)^2}$$

$$\Delta G^*_{c} = \frac{8\pi\sigma_s^{\,2}\sigma_e (T^\circ_{m})^2}{\Delta h_f^{\,2} (T^\circ_{m} - T_x)^2}$$

Here σ is the specific surface free energy of the ordered phase, σ_s and σ_e are the specific surface energies of lamellar crystals with respect to the lateral and folded-chain surfaces, respectively, and Δh_f and Δh_{ODT} are the specific heat at the equilibrium melting point T°_m and at the equilibrium order−disorder transition temperature T°_{ODT}, and T_x is the crystallization temperature. According to the literature,[34,35] σ, σ_s, and σ_e have values of about 1, 10, and 40 erg/cm^2, respectively, and Δh_f and Δh_{ODT} of 200 and 1 J/g, respectively. Assuming $T^\circ_m \approx$ 54 °C and using T_x = 48 °C, the ratio between the two energy barriers should be close to unity for $T^\circ_{\mathrm{ODT}} \approx$ 67 °C. This value is in good agreement with a measurement by Mortensen et al.[20] The values applied for T°_{ODT} and T°_m are both not truly equilibrium values, while in addition σ and Δh_{ODT} are only estimated from related copolymers. Nevertheless, the result of comparable energy barriers is still expected to be reasonably correct.

At small supercooling, the growth is in general nucleation-limited; the small difference between the nucleation barriers for the crystallization and for the order−disorder transition results in a compromise structure. At large supercooling, the nucleation barriers become smaller and do not control the morphology anymore. The thermodynamic driving force ΔG for each of the processes now plays a dominant role. For the order−disorder transition and the crystallization this can be written as

$$\Delta G_{\mathrm{ODT}} = -\Delta h_{\mathrm{ODT}} \frac{T^\circ_{\mathrm{ODT}} - T_x}{T^\circ_{\mathrm{ODT}}}$$

$$\Delta G_c = -\Delta h_f \frac{T^\circ_m - T_x}{T^\circ_m}$$

Because Δh_f is about 2 orders of magnitude larger than Δh_{ODT}, a small decrease of T_x increases $\Delta G_c/\Delta G_{\mathrm{ODT}}$ significantly. The dominant effect of the crystallization shows up at large supercooling. At intermediate levels of supercooling a gradual transition of the morphology can be expected.

The temperature dependence of the final morphologies can be explained on the basis of the above themodynamic argument. Depending on the volume fractions of the PEO and PS blocks, the order−disorder transition is expected to drive the structure toward either hexagonally packed cylinders or a cubic packing of spheres. In contrast, crystallization favors lamellar stacks. At low temperature (below 43 °C), the driving force due to the crystallization is much stronger than that of the order−disorder transition, and a lamellar structure is formed. With increasing temperature, the driving forces for both crystallization and order−disorder transition as well as the difference between them decrease, and the nucleation barriers become very similar. At temperatures between 44 and 47 °C lamellae are still formed, but their perfect arrangement is already destroyed by the order−disorder transition, as indicated by the increase of the fwhm and the decrease in the intensity of the second-order maximum in the SAXS patterns. Around 48 °C, the rates of the two processes become comparable, and their competition leads to the complex structure of the HPL phase. The local balance of the rates of the two processes determines the morphology, and their relative stability influences the perfection of the final structure. As this will not be constant in time, no long correlation length can be expected through this process. This is indeed as observed by SAXS.

In reality, the two nucleation barriers cannot be treated separately, and the coupling of the order−disorder transition and the crystallization will control

the nucleation. The order−disorder transition (induced by fluctuations) and the crystallization taking place in the same temperature range, the fluctuations should enhance the nucleation of crystals. Computer simulations suggest that critical density fluctuations can reduce ΔG^* by about $30k_BT$, which corresponds to an increase of the nucleation rate by a factor as large as 10^{13}.[36] In contrast, microphase separation driven by crystallization also has a low-energy barrier, because the gain in bulk free energy comes not only from the demixing of the two blocks but also from the alignment of the crystallized chains. Further theoretical work and computer simulations are needed to achieve a deeper understanding. In analogy to a theoretical study of the coupling between adsorption and the helix−coil transition,[37] a rich phase diagram is expected.

In conclusion, dynamic coupling and competition between microphase separation and crystallization have been studied in an asymmetric PEO-*b*-PS block copolymer. At large supercooling, crystallization dominates over the microphase separation, resulting in lamellar stacks. With increasing temperature, the order−disorder transition destroys the perfect lamellar arrangement. Finally, at small supercooling, the kinetic rates of these two processes are comparable, and the compromise is a perforated layer phase.

Acknowledgment. The authors thank G. Reiter (Mulhouse, France), and D. Lambreva and I. Sikharulidze (Amsterdam) for valuable discussions. This work is part of the Softlink research program of the "Stichting voor Fundamenteel Onderzoek der Materie (FOM)", which is financially supported by the "Nederlandse Organisatie voor Wetenschappelijk Onderzoek (NOW)".

References and Notes

(1) Muthukumar, M.; Ober, C. K.; Thomas, E. L. *Science* **1997**, *277*, 1225.
(2) Di Marzio, E. A. *Prog. Polym. Sci.* **1999**, *24*, 329.
(3) Hamley, I. W. *The Physics of Block Copolymers*; Oxford University Press: New York, 2000.
(4) Wong, G. C. L.; Commandeur, J.; Fisher, H.; de Jeu, W. H. *Phys. Rev. Lett.* **1996**, *77*, 5221.
(5) Osuji, C.; Zhang, Y.; Mao, G.; Ober, C. K.; Thomas, E. L. *Macromolecules* **1999**, *32*, 7703.
(6) Quiram, D. J.; Register, R. A.; Marchand, G. R.; Adamson, D. H. *Macromolecules* **1998**, *31*, 4891.
(7) Chen, H. L.; Hsiao, S. Ch.; Lin, T. L.; Yamauchi, K.; Hasegawa, H.; Hashimoto, H. *Macromolecules* **2001**, *34*, 671.
(8) Loo, Y. L.; Register, R. A.; Ryan, A. J. *Phys. Rev. Lett.* **2000**, *84*, 4120.
(9) Reiter, G.; Castelein, G.; Sommer, J. U.; Röttele, A.; Thurn-Albrecht, T. *Phys. Rev. Lett.* **2001**, *87*, 226101.
(10) Zhu, L.; Calhoun, B. H.; Ge, Q.; Quirk, R. P.; Cheng, S. Z. D. *Macromolecules* **2001**, *34*, 6649; *Polymer* **2001**, *42*, 5829; *J. Am. Chem. Soc.* **2000**, *122*, 5957.
(11) Bates, F. S.; Fredrickson, G. *Annu. Rev. Phys. Chem.* **1990**, *41*, 525; *Annu. Rev. Mater. Sci.* **1996**, *26*, 501.
(12) Helfand, E.; Wasserman, Z. R. In *Development in Block Copolymers-I*; Goodman, I., Ed.; Applied Science Publishers: London, 1982; Vol. 348, p 99.
(13) Richards, R. W. In *Multicomponent Polymer Systems*; Miles, I. S., Rostami, R., Eds.; John Wiley: New York, 1992; p 103.
(14) Flory, P. J. *Principles of Polymer Chemistry*; Cornell University Press: Ithaca, NY, 1953; Chapter XIII-2.
(15) Gallot, B. *Adv. Polym. Sci.* **1978**, *29*, 85.
(16) Lotz, B.; Kovacs, A. J. *Polym. Prepr.* **1969**, *10*, 820.
(17) Loo, Y. L.; Register, R. A.; Ryan, A. J. *Macromolecules* **2002**, *35*, 2365; **2001**, *34*, 8968.
(18) Zhu, L.; Huang, P.; Chen, W. Y.; Ge, Q.; Quirk, R. P.; Cheng, S. Z. D.; Thomas, E. L.; Lotz, B.; Hsiao, B.; Yeh, F.; Liu, L. *Macromolecules* **2002**, *35*, 3553.
(19) Chen, H. L.; Li, H. C.; Huang, Y. Y.; Chiu, F. C. *Macromolecules* **2002**, *35*, 2417.
(20) Mortensen, K.; Brown, W.; Almdal, K.; Alami, E.; Jada, A. *Langmuir* **1997**, *13*, 3635.
(21) Li, L. B.; Lambrava, D.; de Jeu, W. H., submitted to *J. Macromol. Sci., Part B: Phys.*
(22) Rapp, G.; Gabriel, A.; Dosiere, M.; Koch, M. H. J. *Nucl. Instrum. Methods* **1995**, *A357*, 178.
(23) Koch, M. H. J.; Bordas, J. *Nucl. Instrum. Methods* **1983**, *208*, 461.
(24) Wunderlich, B. *Macromolecular Physics*; Academic Press: New York, 1973; Vol. 2.
(25) Thomas, E. L.; Anderson, D. M.; Henkee, C. S.; Hoffman, D. *Nature* (*London*) **1988**, *334*, 598.
(26) Förster, S.; Khandpur, A. K.; Zhao, J.; Bates, F. S.; Hamley, I. W.; Ryan, A. J.; Bras, W. *Macromolecules* **1994**, *27*, 6922.
(27) Laradji, M.; Shi, A. C.; Desai, R. C.; Noolandi, J. *Phys. Rev. Lett.* **1997**, *78*, 2577.
(28) Qi, S.; Wang, Z. G. *Macromolecules* **1997**, *30*, 4491.
(29) Hajduk, D. A.; Takenouchi, H.; Hillmyer, M. A.; Bates, F. S.; Vigild, M. E.; Almdal, K. *Macromolecules* **1997**, *30*, 3788.
(30) Zhu, L.; et al. *Phys. Rev. Lett.* **2001**, *86*, 6030.
(31) Fredrickson, G. H.; Binder, K. *J. Chem. Phys.* **1989**, *91*, 7265.
(32) Balsara, N. P. *Curr. Opin. Solid State Mater. Sci.* **1999**, *4*, 533.
(33) Schultz, J. M. *Polymer Crystallization*; Oxford University Press: Washington, DC, 2001; Chapter 7.
(34) Floudas, G.; Pakula, T.; Velis, G.; Sioula, S.; Hadjichristidis, N. *J. Chem. Phys.* **1998**, *108*, 6498.
(35) Wu, L.; Lisowski, M.; Talibuddin, S.; Runt, J. *Macromolecules* **1999**, *32*, 1576.
(36) ten Wolde, P. R.; Frenkel, D. *Science* **1997**, *277*, 1975.
(37) Carri, G. A.; Muthukumar, M. *Phys. Rev. Lett.* **1999**, *82*, 5405.

MA025602C